

Article

Working Condition Identification Method of Wind Turbine Drivetrain

Yuhao Huang¹, Huanguo Chen^{1,2,*} , Juchuan Dai³, Hanyu Tao¹ and Xutao Wang¹¹ School of Mechanical Engineering, Zhejiang Sci-Tech University, Hangzhou 310018, China² Zhejiang Province's Key Laboratory of Reliability Technology for Mechanical and Electronic Product, Hangzhou 310018, China³ School of Mechanical Engineering, Hunan University of Science and Technology, Xiangtan 411201, China

* Correspondence: hgchen@zstu.edu.cn

Abstract: The operation state of the wind turbine drivetrain is complex and variable, making it difficult to accurately evaluate under the drivetrain's anomalies. In order to accurately identify the operating state of the main drivetrain, a method for working condition identification is proposed. Firstly, appropriate working condition identification parameters are selected and distinguished from the working condition feature parameters. Secondly, the aerodynamic power prediction model is established, which solves the problem of inaccurate theoretical estimation. Finally, after the historical working conditions are classified, the working condition identification model is established, and the proposed method is analyzed and validated by cases. The results show that the method can accurately identify the working conditions, avoiding the influence of an abnormal state of drivetrain, and provide a basis for real-time state monitoring and evaluation.

Keywords: wind turbine; drivetrain; working conditions; working conditions identification



Citation: Huang, Y.; Chen, H.; Dai, J.; Tao, H.; Wang, X. Working Condition Identification Method of Wind Turbine Drivetrain. *Machines* **2023**, *11*, 495. <https://doi.org/10.3390/machines11040495>

Academic Editors: Davide Astolfi and Antonio J. Marques Cardoso

Received: 22 February 2023

Revised: 5 April 2023

Accepted: 16 April 2023

Published: 20 April 2023



Copyright: © 2023 by the authors. Licensee MDPI, Basel, Switzerland. This article is an open access article distributed under the terms and conditions of the Creative Commons Attribution (CC BY) license (<https://creativecommons.org/licenses/by/4.0/>).

1. Introduction

As a renewable energy, wind energy has broad development prospects with mature technology and large-scale industries, making the stability and reliability of wind turbines the focus of research [1–3]. The wind turbine drivetrain, which is responsible for energy and load transfer, is always in a complex, changeable, and harsh working environment. The downtime caused by the failure of the drivetrain accounts for 40–60% [4], making sense for real-time monitoring and rational adjustment of operation and maintenance arrangement. At present, wind turbines use fixed thresholds to monitor the operating status, which cannot meet the requirements of condition monitoring due to the complexity and diversity of the operating conditions of the drivetrain [5]. Therefore, it is important to classify and accurately identify the working conditions of the drivetrain.

Currently, there are few studies on the classification and identification of working conditions of the drivetrain, and most consider the working condition of the whole wind turbine. Gioia et al. [6] chose rotational speed to discriminate the operating state, dividing the working condition into three states: stopped, energy-generating, and running slip. Yang et al. [7] divided the operating state of the wind turbine into four stages based on the power curve: shutdown stage, maximum wind energy tracking stage, torque control stage, and variable pitch control stage. Gu et al. [8] first used ambient temperature for the initial classification, and then used wind speed to further classify the working conditions of the wind turbine. Hackell et al. [9] classified and identified the operating conditions of the wind turbine by wind speed intervals. Cheng et al. [10] combined wind speed, rotational speed, power, and blade pitch angle with IEC information to classify the operating conditions. Zhao et al. [11] divided the operating states of the wind turbine into seven categories based on wind speed, rotational speed, and blade pitch angle. However, it is difficult to accurately classify and identify the

working conditions of the wind turbine using a single parameter or according to its operating characteristics, and the false alarm rate is high in actual monitoring.

To address this issue, researchers employ multiple parameters based on clustering algorithms for the classification and identification of working conditions. Liu et al. [12] selected power, wind speed, and generator torque as the working condition feature parameters and established a working condition identification model based on the fuzzy C-mean algorithm (FCM). Wang et al. [13] selected wind speed, wind direction, ambient temperature, generator speed, and torque to classify working conditions based on the k-means clustering algorithm, and identified working conditions from the interval ranges of each class. Zheng et al. [14] selected six parameters, including gearbox oil temperature, generator bearing temperature, ambient temperature, active power, wind speed, and generator speed, to form the characteristic parameter set and proposed a method based on particle swarm optimization (PSO) optimized kernel principal component analysis for offshore wind farm operating condition classification. Chen et al. [15] classified and identified the working conditions based on wind speed, cabin angle, blade position, and active power, using a Gaussian mixture model (GMM). Rezamand et al. [16] adopted environmental temperature, wind speed, active power, shaft speed, shaft bearing temperature, generator speed, and generator bearing temperature as the feature set, and used the Kernel Fuzzy C-Means (KFCM) method to divide and identify working conditions. Dong et al. [17] adopted wind speed, blade pitch angle, generator speed, and active power as the feature set, and used k-means clustering to divide working conditions. Although the use of multiple parameters can accurately classify working conditions and reduce the false alarm rate during normal operation, if output parameters (such as active power, generator bearing temperature, generator torque, and so on) are used as working condition identification parameters, they will affect the results of working condition identification when the wind turbine's anomalies occur.

In summary, a working condition identification method for the wind turbine drivetrain is presented. This work guarantees the accuracy of working condition identification while avoiding the influence of the drivetrain's anomalies and provides conditions for real-time monitoring and status evaluation. The overall flowchart is illustrated in Figure 1. The remainder is organized as follows. In Section 2, the working condition identification parameters are selected. In Section 3, an aerodynamic power prediction model is established based on the Long Short-Term Memory (LSTM) algorithm. In Section 4, the working condition identification model is established based on the Light Gradient Boosting Machine (LightGBM) algorithm, and the cases of normal state and abnormal state are selected to validate the proposed method.

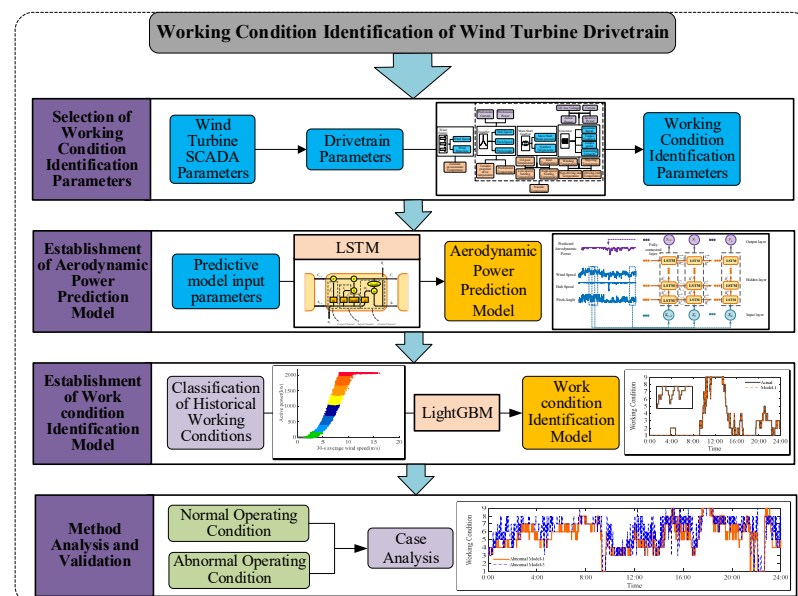


Figure 1. The overall flowchart.

2. Selection of Working Condition Identification Parameters

Researchers typically use working condition feature parameters for real-time condition identification after historical working condition classification. The working condition feature parameters are adopted as working condition identification parameters. When selecting individual input parameters for the wind turbine, such as wind speed or rotor speed, this method does not affect the evaluation results. However, problems arise when selecting multiple working condition feature parameters. Owing to the fact that the working condition feature parameters contain the output of the wind turbine (such as active power, bearing temperature, generator torque, and so on), the results of working condition identification will be affected when the wind turbine has abnormalities or failures. Therefore, it is necessary to distinguish the working condition identification parameters from the working condition feature parameters. The SCADA system collects the whole wind turbine parameters, including blades, generators, grid, etc. [18] The main parameters of the drivetrain are shown in Figure 2.

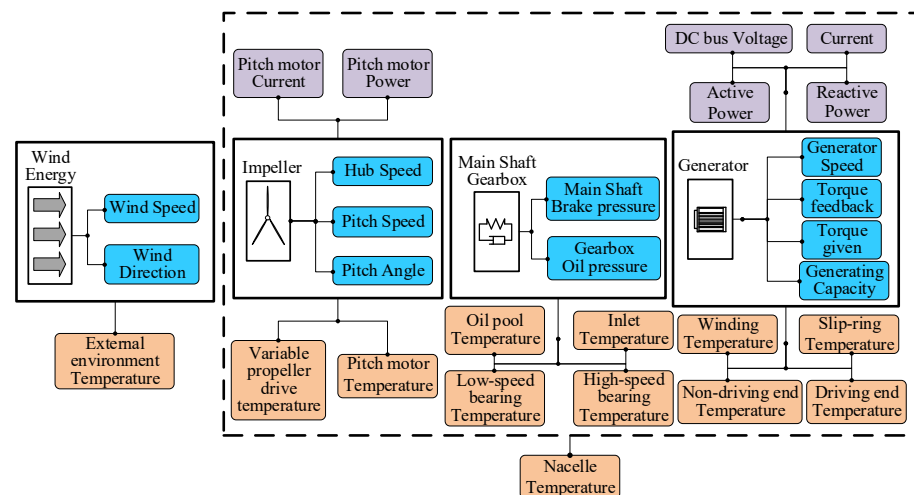


Figure 2. Main parameters of the drivetrain.

In order to accurately classify the historical working conditions of the drivetrain, active power, 30-s average wind speed, hub speed, and ambient temperature are selected as the working condition feature parameters. When the wind turbine is abnormal, according to the control strategy, the wind turbine will adjust the active power by controlling the pitch angle and generator electromagnetic torque. Therefore, if the working condition identification parameters are the same as the working condition characteristic parameters, the active power as the drivetrain output will affect the results of real-time working condition identification. Therefore, it is necessary to select the appropriate working condition identification parameters.

This paper selects aerodynamic power, which is the drivetrain's input, as a substitute for active power as the working condition recognition parameter. The selected working condition identification parameters are aerodynamic power, 30-s average wind speed, hub speed, and ambient temperature.

3. Aerodynamic Power Prediction Model

3.1. Theoretical Calculation of Aerodynamic Power

Aerodynamic power cannot be obtained directly from the wind turbine SCADA system, so it needs to be calculated before the working condition identification. The theoretical aerodynamic power can be calculated from the aerodynamics theory of Betz [19]:

$$P = \frac{1}{2} \rho \pi R^2 V_w^3 C_p \quad (1)$$

where P is the aerodynamic power, ρ is the air density, R is the impeller radius, V_w is the wind speed, and C_p is the rotor power coefficient.

The rotor power coefficient is related to wind speed, hub speed, and pitch angle, which can be calculated by the empirical formula [19]:

$$\begin{cases} C_p = c_1 \left(\frac{c_2}{\gamma} - c_3\beta - c_4\beta^{c_5} - c_6 \right) e^{-\frac{c_7}{\gamma}} \\ \frac{1}{\gamma} = \frac{1}{\lambda + c_8\beta} - \frac{c_9}{\beta^3 + 1} \\ \lambda = \frac{\omega R}{V_w} \end{cases} \quad (2)$$

where $c_1 \sim c_9$ are the wind turbine parameter, β is the pitch angle, γ is the intermediate variable, λ is the speed ratio, ω is the hub speed.

The torque feedback parameters from SCADA data are adopted to calculate the historical aerodynamic power [20]:

$$\begin{cases} T_{in} = iT_{out} \\ P_h = \omega T_{in} \end{cases} \quad (3)$$

where T_{in} is the input torque, T_{out} is the output torque, i is the transmission ratio, P_h is the historical aerodynamic power.

Using data in May 2021, the theoretical calculated aerodynamic power was compared with the actual historical aerodynamic power, as shown in Figure 3. Due to factors such as aging during service, there is a significant discrepancy between theoretical and historical aerodynamic power. Therefore, in order to obtain the actual aerodynamic power, it is necessary to establish an aerodynamic power prediction model.

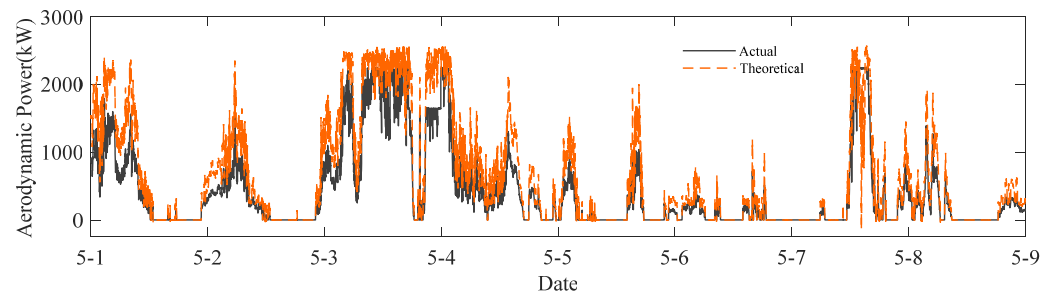


Figure 3. Comparison of theoretical aerodynamic power and historical aerodynamic power.

3.2. LSTM-Based Aerodynamic Power Prediction Model

The LSTM network has shown good performance in solving time-series problems and has demonstrated its excellence in the research of wind turbine power prediction [21–23], state evaluation [24], fault diagnosis [25–27], etc. Therefore, this paper established an aerodynamic power prediction model based on LSTM.

The LSTM is a special type of Recurrent Neural Network (RNN), characterized by its cell state and “gate” structure. It consists of three gating units, the forget gate, the input gate, and the output gate, which preserve and discard information from the sequence data and propagate relevant information along the long chain sequence for prediction [28].

The forget gate is used to determine whether the information will be removed from the memory cell based on the hidden layer state information of the previous moment h_{t-1} . The equation of the forget gate is:

$$f_t = \sigma(W_f[h_{t-1}, x_t] + b_f) \quad (4)$$

The input gate is used to perform updates to the cell state. h_{t-1} and x_t are passed to the activation function σ to update the information. Meanwhile, h_{t-1} and x_t are passed to the function \tanh to obtain the candidate vectors. The equation of the input gate is:

$$i_t = \sigma(W_i[h_{t-1}, x_t] + b_i) \tag{5}$$

$$\tilde{C}_t = \tanh(W_C[h_{t-1}, x_t] + b_C) \tag{6}$$

The cell state is updated by the forgetting gate and the input gate. The equation is:

$$C_t = C_{t-1}f_t + \tilde{C}_ti_t \tag{7}$$

The output gate is used to determine the next hidden layer state information h_t . The equation of the out gate is:

$$o_t = \sigma(W_o[h_{t-1}, x_t] + b_o) \tag{8}$$

$$h_t = o_t \tanh(C_t) \tag{9}$$

where W_f, W_i, W_C, W_o are the corresponding weights, b_f, b_i, b_C, b_o are the corresponding biases, C_{t-1} and C_t are the cell state at moments $t - 1$ and t , respectively.

According to the theoretical aerodynamic power formula, aerodynamic power is related to wind speed, hub speed, and blade pitch angle. Therefore, the 30-s average wind speed, rotor speed, and blade pitch angle selected from the SCADA parameters are used as the input variables of the aerodynamic power prediction model. The model structure is shown in Figure 4.

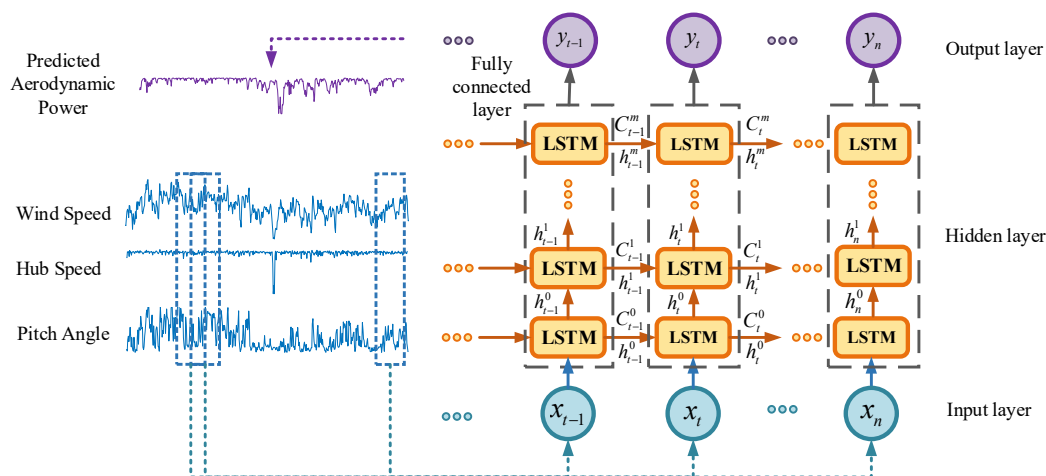


Figure 4. Structure of the aerodynamic power prediction model.

The first layer is the input layer, which sets the memory step length based on the input variables to construct the input time-series data. The second layer is the hidden layer, which passes the time-series features through various LSTM units to mine the coupling relationship between the input variables and the aerodynamic power. Finally, the output layer is connected to the hidden layer through the fully connected layer to obtain the final aerodynamic power prediction result.

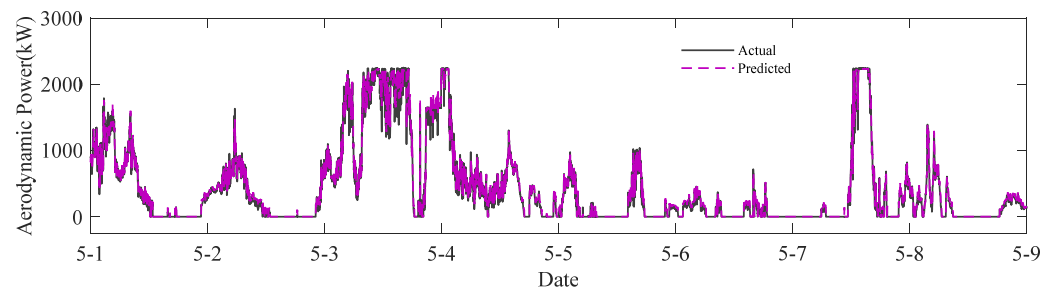
3.3. The Prediction of Aerodynamic Power

Choosing the appropriate number of hidden layers and the number of neuron nodes in each hidden layer is important for constructing the LSTM model. The hyperparameters of the model are adjusted empirically, as shown in Table 1.

Table 1. The hyperparameters of the LSTM model.

Parameter	Value
Hidden layer	3
Time step	20
Iteration cycle	105
Learning rate	0.005
Batch size	64
Loss function	MSE
Optimizer	Adam

The aerodynamic power prediction model was trained and tested using wind turbine data from March to April 2021 and validated using data from May. A total of 88,330 datasets were used, including 62,480 training data samples, 15,620 test data samples, and 10,230 validation data samples. The model has a good prediction effect on aerodynamic power, and the predicted aerodynamic power is closer to the actual aerodynamic power compared with the theoretical aerodynamic power, as shown in Figure 5. The model can provide the accurate actual aerodynamic power for the subsequent working condition identification.

**Figure 5.** Prediction results of the aerodynamic power prediction model.

The mean relative error (MRE) and coefficient of determination R^2 are used to evaluate the prediction model. The equations are:

$$\text{MRE} = \frac{1}{N} \sum_{i=1}^N \left| \frac{y_i - \hat{y}_i}{y_i} \right| \quad (10)$$

$$R^2 = 1 - \frac{\sum_{i=1}^N (y_i - \hat{y}_i)^2}{\sum_{i=1}^N (y_i - \bar{y}_i)^2} \quad (11)$$

where y_i is the actual measured value, \hat{y}_i is the predicted value, \bar{y}_i is the mean value, and N is the number of samples.

The MRE represents the error between the prediction values and actual values. The smaller the MRE, the more the prediction values correspond to the actual values. R^2 characterizes the goodness of fit of the prediction model, while the closer its value is to 1, the better the goodness of fit for the prediction results. The comparison between the theoretical calculation and the model prediction of MRE and R^2 is shown in Table 2. The MRE and R^2 values of the model prediction method are both superior to the theoretical calculation method.

Table 2. Comparison of methods.

Method	MRE	R ²
Theoretical calculation	204.1608843	0.7236284
Model prediction	42.1555041	0.9852787

4. Work Condition Identification Model

4.1. Classification of Historical Working Conditions

The control strategy of the wind turbine will vary depending on the operating conditions. According to the power characteristics and wind speed, the normal operating state can be theoretically divided into five stages (Figure 6): shutdown, start-up (AB), maximum wind energy tracking (BC), constant speed (CD), and constant power (DE) [29].

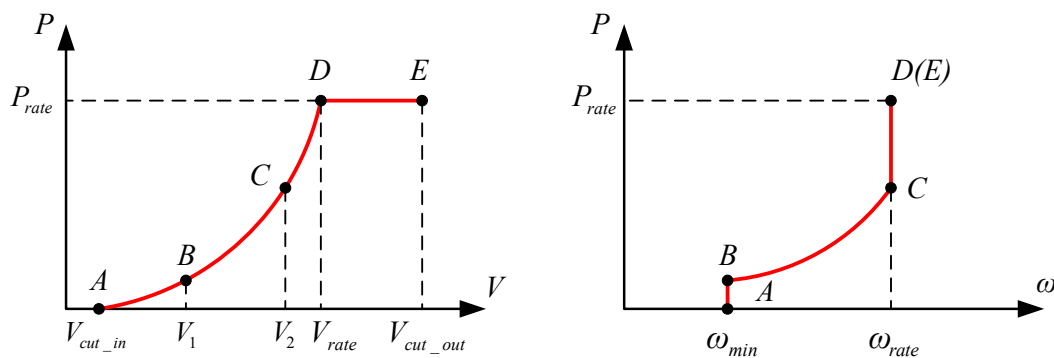


Figure 6. Theoretical working conditions classification.

Firstly, the historical SCADA data of wind turbines are cleaned to remove abnormal values such as power curtailment, outlier, and so on [30]. Then, the operation state is divided into five stages by the power characteristics and wind speed. In view of the large proportion of the maximum wind energy tracking stage and the constant speed stage, the K-means clustering method is used to subdivide the working conditions for these two stages [31]. Considering the influence of environmental factors on the operation status, the active power, 30-s average wind speed, hub speed, and ambient temperature from the SCADA system are selected as feature parameters of working conditions. Finally, the operating state of the drivetrain is divided into 9 types of working conditions (Figure 7).

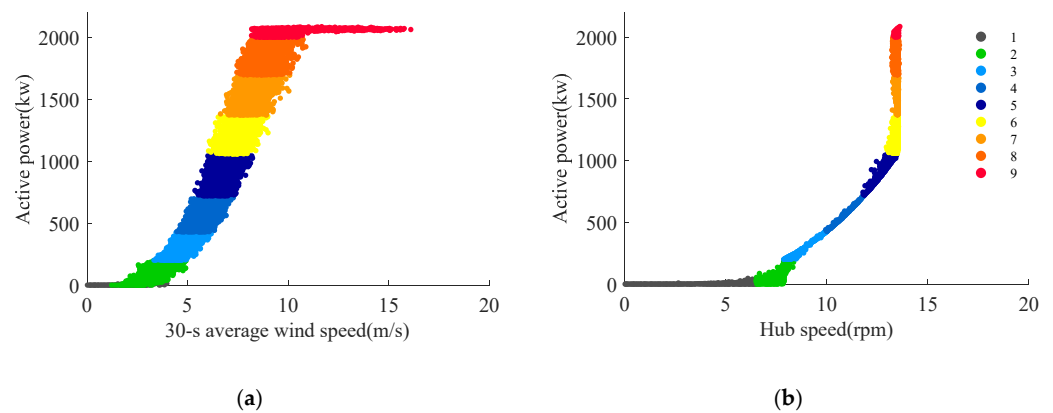


Figure 7. The working condition classification of the drivetrain: (a) 30-s average wind speed vs. active power; (b) hub speed vs. active power.

Working condition 1 is the shutdown stage of the wind turbine, where the wind speed is lower than the cut-in wind speed. Working condition 2 is the start-up stage,

where the wind speed is higher than the cut-in wind speed and the hub speed is limited at the minimum. Working conditions 3 to 5 are clustered by the operational data from the maximum wind energy tracking stage which are designed to capture maximum wind energy. Working conditions 6 to 8 are clustered by the operational data of the constant speed stage, in which the control system regulates the hub speed to keep it at the rated speed value. Working condition 9 is the constant power stage, where the active power is controlled at the rated power value to achieve stable power output.

4.2. LightGBM-Based Working Condition Identification Model

Light Gradient Boosting Machine (LightGBM) is a gradient boosting decision tree (GBDT) framework proposed by Microsoft in 2017. It is a decision tree algorithm proposed based on Gradient One-Side Sampling (GOSS) and Exclusive Feature Binding (EFB), which has the advantages of fast speed, memory saving, and better generalization ability [32]. Therefore, this paper established the working condition identification model based on LightGBM.

Given a supervised learning dataset $X = \{(x_i, y_i)\}_{i=1}^N$, where x represents the sample data and y represents the class label, the objective of the LightGBM algorithm is to find a mapping relation $\hat{F}(x)$ that approximates the function $F(x)$ while minimizing the loss function $\Psi(y, F(x))$:

$$\hat{F} = \operatorname{argmin}_F E_{y,x} \Psi(y, F(x)) \tag{12}$$

The objective function $Obj^{(t)}$ can be represented as:

$$Obj^{(t)} = \sum_{i=1}^n \Psi(y_i, F_{t-1}(x_i) + f_t(x_i)) + \sum_k \Omega(f_k) \tag{13}$$

where $\Omega(f_k)$ is the regular term.

The Newton method is used in LightGBM to quickly approximate the objective function:

$$Obj^{(t)} \cong \sum_{i=1}^n \left[g_i f_t(x_i) + \frac{1}{2} h_i f_t^2(x_i) \right] + \sum_k \Omega(f_k) \tag{14}$$

where g_i is the first-order loss function and h_i is the second-order loss function.

$$g_i = \partial_{F_{t-1}(x_i)} \Psi(y_i, F_{t-1}(x_i)) \tag{15}$$

$$h_i = \partial_{F_{t-1}(x_i)}^2 \Psi(y_i, F_{t-1}(x_i)) \tag{16}$$

The information gain is defined as:

$$G = \frac{1}{2} \left[\frac{(\sum_{i \in I_L} g_i)^2}{\sum_{i \in I_L} h_i + \lambda} + \frac{(\sum_{i \in I_R} g_i)^2}{\sum_{i \in I_R} h_i + \lambda} - \frac{(\sum_{i \in I} g_i)^2}{\sum_{i \in I} h_i + \lambda} \right] \tag{17}$$

The working condition identification parameters are used as the input data, and the sub-conditions classified by the historical working condition classification are used as the class labels. The working condition identification model is established based on the LightGBM algorithm, and the process flow chart is shown in Figure 8.

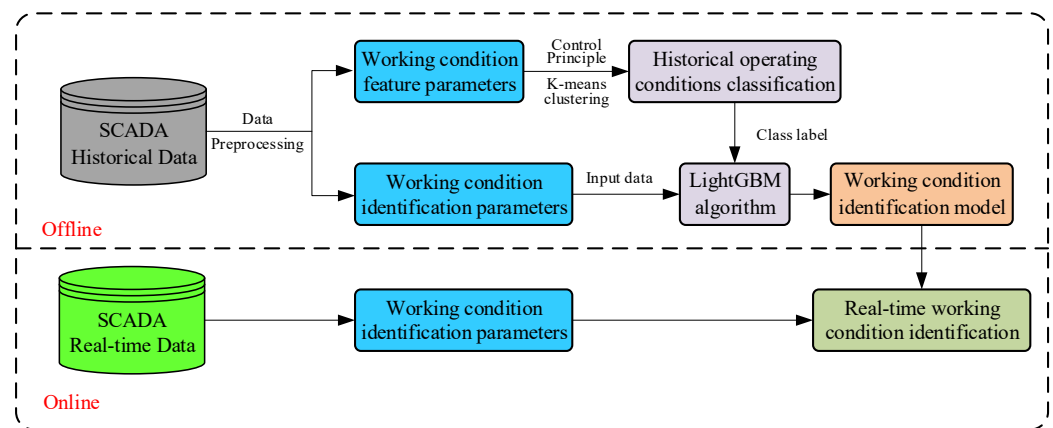


Figure 8. Flow chart of the work condition identification.

4.3. Working Condition Identification under Normal Operation State

The working condition identification model is established according to the working condition identification parameters. The working condition identification parameters of the three working condition identification models are as follows:

- (1) Model-1: active power, 30-s average wind speed, hub speed, and ambient temperature.
- (2) Model-2: 30-s average wind speed, hub speed, and ambient temperature.
- (3) Model-3: aerodynamic power, 30-s average wind speed, hub speed, and ambient temperature.

The data from 7 May 2021 were used as a normal operation state case; the active power-wind speed diagram is shown in Figure 9a. Model-1 can accurately identify the working conditions, but its use of active power as input will affect the working condition identification when the drivetrain is abnormal, which will be demonstrated later (Figure 9b). Model-2 has difficulty in accurately identifying the working conditions, especially in working conditions 6 to 9 (Figure 9c). The reason is that the hub speed fluctuates at the maximum speed value during the constant speed stage and the constant power stage, while the ambient temperature has a low correlation with the operating state. Therefore, only the 30-s average wind speed is used to identify the working conditions in these two phases, which results in low identification accuracy. Model-3 adopts aerodynamic power instead of active power as the working condition identification parameter, and the identification results are also relatively accurate (Figure 9d). This model can ensure identification accuracy while avoiding wind turbine abnormalities affecting the working condition identification results.

Accuracy rate and $F1_Score$ are used as indicators to evaluate the working condition identification model. The calculation formula is as follows:

$$Acc = \frac{TP + TN}{TP + TN + FP + FN} \quad (18)$$

$$\begin{cases} Pec = \frac{TP}{TP + FP} \\ Rec = \frac{TP}{TP + FN} \\ F1 = \frac{2 \times Pec \times Rec}{Pec + Rec} \end{cases} \quad (19)$$

where Acc is accuracy rate, Pec is the precision, Rec is the recall, $F1$ is the $F1_Score$, TP is the true positives, TN is the true negatives, FP is the false positives, FN is the false negatives.

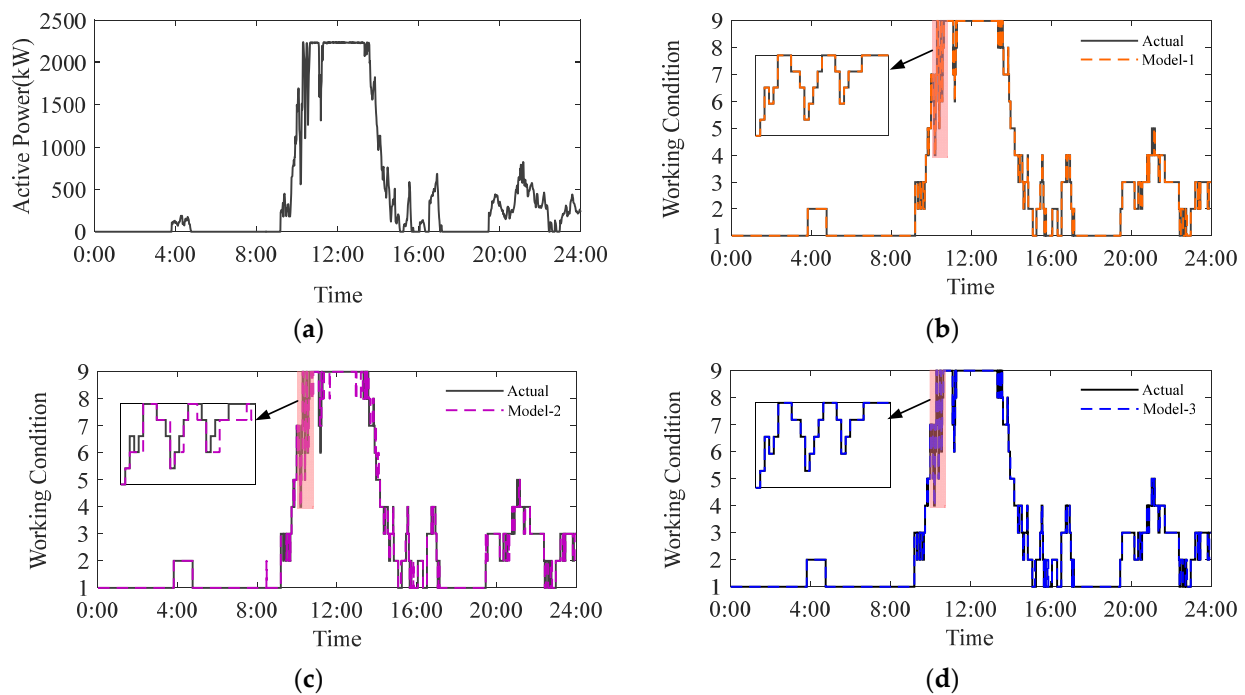


Figure 9. The results of the working condition identification: (a) active power vs. wind speed on May 7, 2021; (b) the results of model-1; (c) the results of model-2; (d) the results of model-3.

The accuracy rate is the proportion of the number of correctly classified samples to the total number of samples, while the closer its value is to 1, the better the classification is. Precision is the proportion of samples that are actually positive out of all samples predicted as positive. Recall is the proportion of samples that are predicted as positive out of all actual positive samples. $F1_Score$ is the harmonic mean of precision and recall, and the higher the value, the more effective the classification. For multi-class problems, we consider them as a combination of multiple binary classification models. The $F1_Score$ under each class is calculated for unweighted average to evaluate the model. The accuracy rate and the average of $F1_Score$ of the different working conditions identification models are shown in Table 3. Model-1 and Model-3 have higher accuracy rate and average of $F1_Score$, and the effective is better. Model-2 has lower accuracy rate and the average of $F1_Score$ than the other two models, indicating poor performance.

Table 3. Evaluation results of different working conditions identification models.

Model	Acc	Average_F1
Model-1	0.9973284	0.9960851
Model-2	0.9242778	0.8446969
Model-3	0.9900651	0.9835994

4.4. Working Condition Identification under Abnormal Operation State

The wind turbine experienced multiple generator non-drive temperature overrun faults and the generator bearing high-temperature warnings on 16 March 2022, followed by shutdown for maintenance (Figure 10). The data from 16 March 2022 were used as an abnormal operation state case.

No.	Wind turbine	Catego	Cod	Tags	Occurrence time	Recovery time	Fault Descriptopn
180	537#	Warning	295	A_GeneratorBearingToc	2022-03-16 08:59:48	2022-03-16 09:23:44	Generator bearing high temperature warning
181	537#	Fault	175	A_GeneratorNonDriveE	2022-03-16 09:16:57	2022-03-16 09:34:19	Generator non-drive end temperature over limit fault
182	537#	Warning	295	A_GeneratorBearingToc	2022-03-16 21:06:55	2022-03-16 22:10:14	Generator bearing high temperature warning
183	537#	Fault	175	A_GeneratorNonDriveE	2022-03-16 21:27:26	2022-03-16 21:30:13	Generator non-drive end temperature over limit fault
184	537#	Fault	175	A_GeneratorNonDriveE	2022-03-16 21:44:16	2022-03-16 21:16:59	Generator non-drive end temperature over limit fault
185	537#	Fault	175	A_GeneratorNonDriveE	2022-03-16 22:03:42	2022-03-16 22:37:07	Generator non-drive end temperature over limit fault
186	537#	Fault	110	A_ScadaShutdownRequ	2022-03-16 22:37:02	2022-03-16 22:37:03	Remote monitoring shutdown

Figure 10. Wind turbine operation logs.

The result of the aerodynamic power prediction model for abnormal operation state of the wind turbine is shown in Figure 11. Compared with the results of the aerodynamic power prediction model for normal operation state (Figure 5), there is a significant residual between the predicted and the aerodynamic power calculated by torque feedback parameter in Equation (3). When the drivetrain is abnormal, as one of the outputs, the torque feedback parameter can be affected, which leads to inaccurate calculation of aerodynamic power. Therefore, the output parameters in SCADA will be affected when wind turbine abnormalities occur. It also shows that the actual aerodynamic power cannot be calculated from Equation (3) but needs to be predicted by adopting the aerodynamic power prediction model.

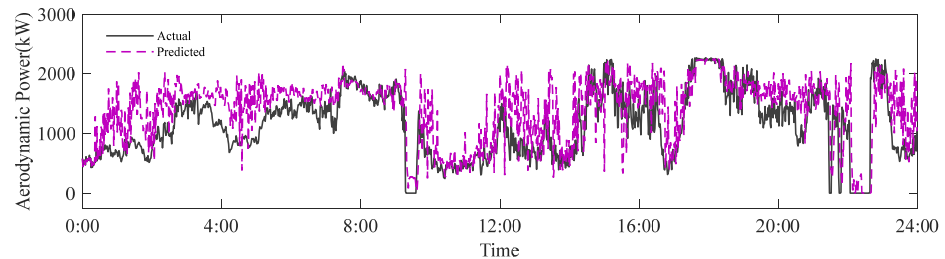


Figure 11. The result of the aerodynamic power prediction model on 16 March 2022.

If Model-3 uses the predicted aerodynamic power from the aerodynamic power prediction model as the actual aerodynamic power, the comparison result of its working condition identification under normal operation state with Model-1 is shown in Figure 12a. The results of Model-3 using predicted aerodynamic power for working condition identification have reduced accuracy compared with the results of calculating aerodynamic power using Equation (3). The reason is that the accuracy of the aerodynamic power prediction model is not high enough, which causes the misjudgment of the working condition identification model.

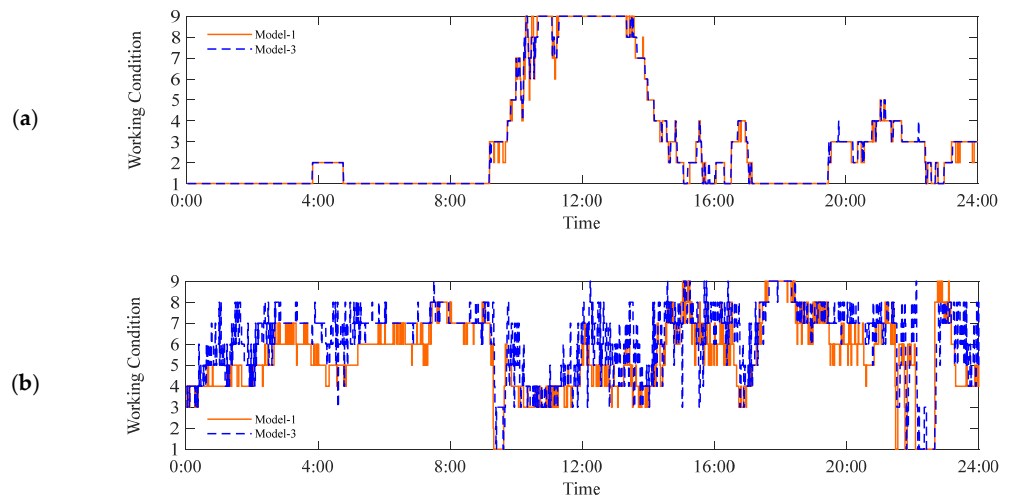


Figure 12. The comparison results of Model-3 and Model-1: (a) under normal operation state; (b) under abnormal operation state.

The comparison results of Model-3 and Model-1 under abnormal operating state are shown in Figure 12b. Compared with the normal operation state of wind turbines, it is obvious that the misjudgment rate of working condition identification increases. Thus, when the drivetrain output (active power) is used as the working condition identification parameter, it is difficult to identify the working condition accurately under the abnormal operating state. The method proposed in this paper, which uses the input (aerodynamic power) as the working condition identification parameter, can avoid this problem while ensuring accuracy.

5. Conclusions

In order to avoid the effect of abnormal operation state on the working conditions identification and accurately identify the real-time working conditions, a working condition identification method of the wind turbine drivetrain is proposed, and it is applied to an actual wind turbine to verify its feasibility. The results showed that:

(1) Theoretical method cannot accurately calculate the actual aerodynamic power of the drivetrain due to the wind turbine aging and other reasons. The LSTM-based aerodynamic power prediction model proposed can accurately predict the actual aerodynamic power.

(2) Adopting aerodynamic power instead of active power as the working condition identification parameter can guarantee the accuracy of working condition identification while avoiding the impact of the drivetrain's anomalies.

(3) The accuracy of the aerodynamic power prediction model will affect the judgment result of the working condition identification model. In the future, the performance of the aerodynamic power prediction model needs to be further improved through more data and more optimized algorithms.

Author Contributions: Conceptualization, Y.H.; methodology, Y.H.; validation, Y.H. and H.C.; formal analysis, X.W.; investigation, Y.H. and H.T.; resources, J.D.; data curation, H.T.; writing—original draft preparation, Y.H.; writing—review and editing, Y.H., H.C., and J.D.; project administration, H.C.; funding acquisition, H.C. All authors have read and agreed to the published version of the manuscript.

Funding: This research was funded by the National Natural Science Foundation of the People's Republic of China (grant number 51975535 and 52075164), the Key R & D Projects of Zhejiang Province (grant number 2021C01133).

Institutional Review Board Statement: Not applicable.

Informed Consent Statement: Not applicable.

Data Availability Statement: The data presented in this study are available on request from the corresponding author. The data are not publicly available due to business privacy.

Conflicts of Interest: The authors declare that they have no conflicts of interest.

References

1. Chu, S.; Majumdar, A. Opportunities and Challenges for a Sustainable Energy Future. *Nature* **2012**, *488*, 294–303. [[CrossRef](#)] [[PubMed](#)]
2. Astolfi, D. Perspectives on SCADA Data Analysis Methods for Multivariate Wind Turbine Power Curve Modeling. *Machines* **2021**, *9*, 100. [[CrossRef](#)]
3. Tchakoua, P.; Wamkeue, R.; Ouhrouche, M.; Slaoui-Hasnaoui, F.; Tameghe, T.A.; Ekemb, G. Wind Turbine Condition Monitoring: State-of-the-Art Review, New Trends, and Future Challenges. *Energies* **2014**, *7*, 2595–2630. [[CrossRef](#)]
4. Ribrant, J.; Bertling, L.M. Survey of Failures in Wind Power Systems With Focus on Swedish Wind Power Plants During 1997–2005. *IEEE Trans. Energy Convers.* **2007**, *22*, 167–173. [[CrossRef](#)]
5. Shi, W.; Wang, F.; Zhuo, Y.; Liu, Y. Research on Operation Condition Classification Method for Vibration Monitoring of Wind Turbine. In Proceedings of the 2010 Asia-Pacific Power and Energy Engineering Conference, Chengdu, China, 28–31 March 2010; pp. 1–6.
6. Gioia, N.; Peeters, C.; Guillaume, P.; Helsen, J. Identification of Noise, Vibration and Harshness Behavior of Wind Turbine Drivetrain under Different Operating Conditions. *Energies* **2019**, *12*, 3401. [[CrossRef](#)]

7. Yang, T.; Zhao, L.; Xu, J.; Li, W.; Zhang, G. Abnormal Identification Method of Wind Power Turbine Based on Copula Function. *Electr. Switch.* **2021**, *59*, 26–31.
8. Gu, Y.; Su, L.; Zhong, Y.; Xu, T. An Online Fault Early Warning Method for Wind Turbine Gearbox Based on Operational Condition Division. *Electr. Power Sci. Eng.* **2014**, *30*, 1–5+11.
9. Hackell, M.W.; Rolfes, R.; Kane, M.B.; Lynch, J.P. Three-Tier Modular Structural Health Monitoring Framework Using Environmental and Operational Condition Clustering for Data Normalization: Validation on an Operational Wind Turbine System. *Proc. IEEE* **2016**, *104*, 1632–1646. [[CrossRef](#)]
10. Cheng, H.; Zhang, Q. Multidimensional wind turbine operating condition identification based on operating data. In Proceedings of the 6th China Wind Power Aftermarket Exchange and Cooperation Conference, Beijing, China, 21–24 October 2019; pp. 42–47.
11. Zhao, Y.; Pan, J.; Huang, Z.; Miao, Y.; Jiang, J.; Wang, Z. Analysis of Vibration Monitoring Data of an Onshore Wind Turbine under Different Operational Conditions. *Eng. Struct.* **2020**, *205*, 110071. [[CrossRef](#)]
12. Liu, C.; Yan, X. Monitoring of the State of the Gear Box of a Wind Power Generator Unit Based on the Operating Condition Identification. *J. Eng. Therm. Energy Power* **2016**, *31*, 41–46+133. [[CrossRef](#)]
13. Wang, H.; Wang, H.; Jiang, G.; Li, J.; Wang, Y. Early Fault Detection of Wind Turbines Based on Operational Condition Clustering and Optimized Deep Belief Network Modeling. *Energies* **2019**, *12*, 984. [[CrossRef](#)]
14. Zheng, X.; Li, M.; Wang, J.; Ren, H.; Fu, Y. Operational conditions classification of offshore wind turbines based on kernel principal analysis optimized by PSO. *Power Syst. Prot. Control* **2016**, *44*, 28–35. [[CrossRef](#)]
15. Chen, H.; Ma, H.; Chu, X.; Xue, D. Anomaly Detection and Critical Attributes Identification for Products with Multiple Operating Conditions Based on Isolation Forest. *Adv. Eng. Inform.* **2020**, *46*, 101139. [[CrossRef](#)]
16. Rezamand, M.; Kordestani, M.; Orchard, M.E.; Carriveau, R.; Ting, D.S.-K.; Saif, M. Improved Remaining Useful Life Estimation of Wind Turbine Drivetrain Bearings Under Varying Operating Conditions. *IEEE Trans. Ind. Inform.* **2021**, *17*, 1742–1752. [[CrossRef](#)]
17. Dong, Y.; Li, Y.; Cao, H.; He, C.; Gu, Y. Real-time Health Condition Evaluation on Wind Turbines Based on Operational Condition Recognition. *Proc. CSEE* **2013**, *33*, 88–95+15. [[CrossRef](#)]
18. Zeng, H.; Dai, J.; Zuo, C.; Chen, H.; Li, M.; Zhang, F. Correlation Investigation of Wind Turbine Multiple Operating Parameters Based on SCADA Data. *Energies* **2022**, *15*, 5280. [[CrossRef](#)]
19. Sloomweg, J.G.; Polinder, H.; Kling, W.L. Representing Wind Turbine Electrical Generating Systems in Fundamental Frequency Simulations. *IEEE Trans. Energy Convers.* **2003**, *18*, 9. [[CrossRef](#)]
20. Qin, D.; Tian, M.; Yang, J. Study on Dynamic Characteristics of Gear Transmission System of Wind Generator under Various Wind Load. *Acta Energ. Sol. Sin.* **2012**, *33*, 190–196.
21. Li, Z.; Luo, X.; Liu, M.; Cao, X.; Du, S.; Sun, H. Short-Term Prediction of the Power of a New Wind Turbine Based on IAO-LSTM. *Energy Rep.* **2022**, *8*, 9025–9037. [[CrossRef](#)]
22. Zhang, J.; Yan, J.; Infield, D.; Liu, Y.; Lien, F. Short-Term Forecasting and Uncertainty Analysis of Wind Turbine Power Based on Long Short-Term Memory Network and Gaussian Mixture Model. *Appl. Energy* **2019**, *241*, 229–244. [[CrossRef](#)]
23. Li, J.; Song, Z.; Wang, X.; Wang, Y.; Jia, Y. A Novel Offshore Wind Farm Typhoon Wind Speed Prediction Model Based on PSO-Bi-LSTM Improved by VMD. *Energy* **2022**, *251*, 123848. [[CrossRef](#)]
24. Zhu, Y.; Zhu, C.; Tan, J.; Wang, Y.; Tao, J. Operational State Assessment of Wind Turbine Gearbox Based on Long Short-Term Memory Networks and Fuzzy Synthesis. *Renew. Energy* **2022**, *181*, 1167–1176. [[CrossRef](#)]
25. Lei, J.; Liu, C.; Jiang, D. Fault Diagnosis of Wind Turbine Based on Long Short-Term Memory Networks. *Renew. Energy* **2019**, *133*, 422–432. [[CrossRef](#)]
26. Chen, H.; Liu, H.; Chu, X.; Liu, Q.; Xue, D. Anomaly Detection and Critical SCADA Parameters Identification for Wind Turbines Based on LSTM-AE Neural Network. *Renew. Energy* **2021**, *172*, 829–840. [[CrossRef](#)]
27. Zhang, C.; Hu, D.; Yang, T. Anomaly Detection and Diagnosis for Wind Turbines Using Long Short-Term Memory-Based Stacked Denoising Autoencoders and XGBoost. *Reliab. Eng. Syst. Saf.* **2022**, *222*, 108445. [[CrossRef](#)]
28. Graves, A. Long Short-Term Memory. In *Supervised Sequence Labelling with Recurrent Neural Networks*; Springer: Berlin/Heidelberg, Germany, 2012; pp. 37–45. [[CrossRef](#)]
29. Li, C.; Ye, Z.; Gao, W.; Jiang, Z. *Modern Large-Scale Wind Turbine Design Principle*, 1st ed.; Shanghai Scientific & Technical Publishers: Shanghai, China, 2013.
30. Morrison, R.; Liu, X.; Lin, Z. Anomaly Detection in Wind Turbine SCADA Data for Power Curve Cleaning. *Renew. Energy* **2022**, *184*, 473–486. [[CrossRef](#)]
31. Chen, H.; Xie, C.; Dai, J.; Cen, E.; Li, J. SCADA Data-Based Working Condition Classification for Condition Assessment of Wind Turbine Main Transmission System. *Energies* **2021**, *14*, 7043. [[CrossRef](#)]
32. Ke, G.; Meng, Q.; Finley, T.; Wang, T.; Chen, W.; Ma, W.; Ye, Q.; Liu, T. A highly efficient gradient boosting decision tree. In Proceedings of the Advances in Neural Information Processing Systems, Long Beach, CA, USA, 4–9 December 2017; pp. 3146–3154.

Disclaimer/Publisher’s Note: The statements, opinions and data contained in all publications are solely those of the individual author(s) and contributor(s) and not of MDPI and/or the editor(s). MDPI and/or the editor(s) disclaim responsibility for any injury to people or property resulting from any ideas, methods, instructions or products referred to in the content.